Effects of Dilution and Pressure on Detonation Propagation across an Inert Layer

Journal:	*AIAA Journal*
Manuscript ID	2022-08-J062397.R1
Manuscript Type:	Regular Article
Date Submitted by the Author:	19-Nov-2022
Complete List of Authors:	Wang, Yuan; College of Engineering Su, Jingyi; College of Engineering Deiterding, Ralf; University of Southampton, Aerodynamics and Flight Mechanics Research Group Chen, Zheng; Peking University, Mechanical Engineering
Subject Index Category:	60310 Detonation < 60000 PROPULSION
Select ONE Subject Index for the Table of Contents. This is where your paper will show up in the Table of Contents:	60000 PROPULSION

Effects of Dilution and Pressure on Detonation Propagation across an Inert Layer

Yuan Wang,[1] and Jingyi Su[2]
CAPT, SKLTCS, BIC-ESAT, College of Engineering, Peking University, Beijing 100871, China

Ralf Deiterding[3]
Aerodynamics and Flight Mechanics Research Group, University of Southampton, Southampton SO16 7QF, United Kingdom

and
Zheng Chen[4]
CAPT, SKLTCS, BIC-ESAT, College of Engineering, Peking University, Beijing 100871, China

In explosion accidents, inert layer(s) can be used to dampen or suppress detonation propagation. In detonation engines, the detonation may propagate in an inhomogeneous mixture with inert layer(s). Here the detonation propagation in hydrogen/oxygen/nitrogen mixtures with a single inert layer normal to the detonation propagation direction was investigated. Six hydrogen/oxygen/nitrogen mixtures with different amounts of nitrogen dilution and at different initial pressures were considered. The emphasis was placed on assessing the effects of nitrogen dilution and pressure on detonation across an inert layer. It was found that successful detonation reinitiation occurs only when the inert layer thickness is below some critical value. The detonation reinitiation process was analyzed. The interactions of transverse waves, reactive-inert layer interface and instabilities jointly induce local autoignition/explosions and detonation reinitiation. Counterintuitively, it was found that a thicker inert layer is required to quench a weaker detonation (with more nitrogen dilution or with lower energy density at lower pressure). With the increase of nitrogen dilution or decrease of initial pressure, the induction length and cell size of the detonation become larger, which unexpectedly results in the larger critical inert layer thickness.

[1] Graduate Student, College of Engineering.
[2] Graduate Student, College of Engineering
[3] Professor, Aerodynamics and Flight Mechanics Research Group.
[4] Professor, College of Engineering.

I. Introduction

As a zero-carbon-emission fuel, hydrogen has recently drawn significant attention due to its promising applications in energy storage and energy conversion [1]. Great effort has been devoted to investigating the properties of hydrogen flames and detonations (e.g., [2-8]). However, there is still severe safety concern for hydrogen storage and utilization since hydrogen is easily to be ignited [9-11]. It is well known that accidental explosion can cause extremely severe damage if detonation occurs. One way to reduce the damage is to dampen or suppress detonation propagation in combustible gases using inert zones or inert layers. Transition of detonation across an inert region might induce detonation quenching and reinitiation. Besides, hydrogen is popularly used in rotating detonation engines (RDEs). In RDEs, hydrogen and air may not be perfectly mixed and burned mixture can appear in front of the detonation front. Therefore, understanding detonation propagation and quenching in inhomogeneous hydrogen/oxygen/diluent mixtures is of crucial importance for controlling explosion and developing detonation engines. In the literature, there are many studies on detonation propagation in inhomogeneous mixtures (see [12] and references therein). In this work, we specifically focus on the transition of gaseous detonation across a single inert layer normal to the detonation propagation direction in different $H_2/O_2/N_2$ mixtures.

There are several experimental or numerical studies on/related to detonation propagation across a single or multiple inert layers. For examples, Teodorczyk and Benoan [13] studied detonation reinitiation after the interaction of detonation with an inert zone. Bull et al. [14] investigated detonation propagation in ethylene/air and propane/air mixtures with an inert zone consisting of pure air. They measured the critical size of the inert zone and the transition distance for detonation reinitiation. Bjerketvedt et al. [15] conducted experiments on detonation reinitiation across a single inert region and assessed different factors affecting the detonation reinitiation. Tropin and Bedarev [16] investigated numerically detonation suppression by an inert layer with different inert gases. They found that carbon dioxide is more efficient for suppressing the detonation wave than nitrogen and argon. Tang-Yuk et al. [17] simulated detonation transmission across an inert layer and found that the critical inert layer thickness for the two-dimensional (2D) case is one order larger than that for the one-dimensional (1D) case. In our recent study[18], detonation propagation across multiple inert layers was simulated and a double cellular structure was observed and interpreted. The size of the large cellular structure was found to be linearly proportional to the inert layer spacing.

Though detonation propagation across inert layer(s) was investigated in studies mentioned above, the reinitiation mechanism and the dependence of critical inert layer thickness on mixture composition and thermal conditions are

still not well understood. This motivates the present study, whose objectives are two-fold: (1) to interpret the mechanism and critical condition for detonation reinitiation after it is quenched by an inert layer and (2) to assess the effects of nitrogen dilution and pressure on detonation across an inert layer. We shall consider detonation propagation in different $H_2/O_2/N_2$ mixtures with a single inert layer normal to the detonation propagation direction. A single inert layer instead of multiple inert layers is considered here so that complicated interactions between detonation and multiple inert layers are prevented and thereby the detonation reinitiation mechanism can be clearly interpreted. Both 1D and 2D simulations are conducted. Detailed chemistry is considered in all simulations.

In the following sections, the model and the numerical methods are introduced first. Then, the results from 1D and 2D simulations are presented and detonation reinitiation as well as its dependence on dilution and pressure is discussed. Finally, the conclusions are summarized.

II. Model and Numerical Methods

The model is depicted in Fig. 1. The detonation propagates into a static, homogeneous, stoichiometric $H_2/O_2/N_2$ mixture, which is separated by an inert layer of pure nitrogen. The inert layer starts at $x = 0$ cm and ends at $x = a$. The ZND detonation structure with the induction length of l_i is used to initiate the detonation propagating to the right side. For the 2D case, the detonation cellular structure fully develops before the detonation enters the inter layer.

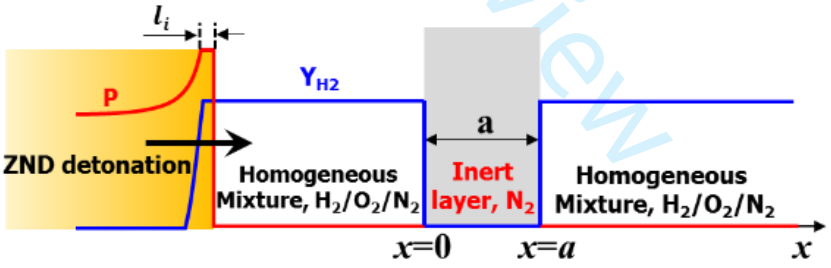

Fig. 1. Schematic of the initial pressure and hydrogen mass fraction distributions.

The detonation is quenched after entering the inert layer and the leading shock is attenuated during its propagation across it. When the inert layer thickness is below some critical value, denoted as a_c, the detonation can be reinitiated by the transmitted shock. The critical inert layer thickness, a_c, is expected to be related to the induction length l_i and the detonation cell size λ, respectively for 1D and 2D detonations. Note that the induction length and the cell size is obtained respectively from the present 1D and 2D simulations. To change l_i and λ, we considered different

stoichiometric $H_2/O_2/N_2$ mixtures (whose molar ratio is $H_2:O_2:N_2 = 2:1:s$) with different amounts of N_2 dilution of s = 3.76, 5, 6 and 7 and at different initial pressures of P_0 = 15, 30 and 60 KPa (see table 1).

Table 1: The composition, initial temperature and pressure, induction length and detonation cell size of six mixtures.

No.	$H_2:O_2:N_2$	T_0 /K	P_0 /kPa	l_i /mm	λ/mm
1	2:1:3.76	300	15	1.49	12
2	2:1:5	300	15	2.22	14.3
3	2:1:6	300	15	3.08	20
4	2:1:7	300	15	4.31	25
5	2:1:7	300	30	2.23	13.3
6	2:1:7	300	60	1.29	7.5

Table 1 lists six mixtures considered in this work. The induction length l_i and detonation cell size λ for these mixtures are also listed in Table 1. The induction length is defined as the distance from the leading shock wave to the position where maximum thermicity appears. The cell size is the vertical length of the regular detonation cell structure. As expected, Table 1 shows that increasing nitrogen dilution and reducing initial pressure both can greatly increase the induction length and detonation cell size.

The in-house codes A-SURF [19, 20] and AMROC [21, 22], were used to simulate 1D and 2D detonation propagating across an inert layer, respectively. Both codes solve the Navier-Stokes equations for unsteady, compressible, multi-component, reactive flow using the finite volume method. The HLLC or hybrid Roe-HLL Riemann solver for mixtures of thermally perfect gases was used to calculate the convective fluxes. The second-order accurate central difference scheme was used for multi-species diffusion terms. The detailed kinetic model for hydrogen oxidation developed by Li et al. [23] was used in all simulations. The CHEMKIN package was employed to evaluate the reaction rates and thermodynamic properties. Both A-SURF and AMROC have been successfully used in previous studies on detonation propagation (e.g., [24-30]). The details on the governing equations, numerical methods and code validation of A-SURF and AMROC can be found in [19-21] and thereby are not repeated here.

Transmissive boundary conditions were used for the left and right sides in both 1D and 2D computational domains. Periodic boundary conditions were used for the top and bottom sides in the 2D simulations. Therefore, the effects of any boundary layer and its interaction with shock waves were not considered here. Note that in practice detonation propagates in a finite domain with physical confinement rather than in an infinite domain with periodic boundary conditions. This study focused on the effect of single inert layer and thereby the confinement effect was not considered

here for simplicity. In future works, it would be interesting to take into account the confinement effect.

The length and width of the computational domain are large enough for detonation propagation and formation of a steady cellular structure. To accurately and efficiently resolve the transient process, dynamically adaptive mesh refinement was used in both 1D and 2D simulations. Mesh refinement was based on local gradients of temperature, density and pressure. The finest mesh size is 7.8 μm. Since the smallest induction length is l_i = 1.29 mm, there are more than 165 grid points within one induction length. Our numerical tests indicated that the conclusions remain the same when the finest mesh size is halved. Compared to present work, some studies [31, 32] shows that the relatively coarser mesh resolutions were able to adequately capture the detonation wave dynamics in detonation engines.

III. Results and Discussion

Both 1D and 2D simulations were conducted. In practice, the detonation propagation process is intrinsically multi-dimensional. Therefore, 1D simulation cannot reveal the real dynamics of the detonation wave. Nevertheless, the 1D simulation is still helpful to understand the coupling between the lead shock and the reactions at least in a qualitatively manner. Therefore, results from 1D simulation are first presented and discussed below.

A. One-dimensional Detonation Propagation

First, we considered 1D detonation propagating across an inert layer for the six mixtures listed in Table 1. Only the results for mixture 1 and mixture 4 are shown in Fig. 2. The vertical dashed lines represent the left and right boundaries of the inert layer at $x = 0$ and $x = a$.

In simulation, the shock position is determined based on the maximum pressure gradient, and the shock speed is obtained via numerical differentiation of the shock position with respect to time. Figure 2(a) shows that the shock speed decays rapidly after it enters the inert layer starting at $x = 0$ cm. Within the inert layer, the shock speed decreases from the CJ detonation speed D_{CJ} = 1695 m/s to 1578 m/s (i.e., $0.93D_{CJ}$) for a = 5 mm and to 1521 m/s (i.e., $0.90D_{CJ}$) for a = 8 mm, respectively. Successful detonation reinitiation is achieved only for a = 5, 6 and 7 mm. Similar to the direct detonation initiation observed in previous studies (e.g., [33-35]), for successful detonation reinitiation, an overdriven detonation develops after a rapid decrease in the leading shock speed. Then the overdriven detonation decays toward the CJ detonation. With the increase of inert layer thickness, the position for successful detonation reinitiation and the maximum speed of the overdriven detonation both become larger. However, further increasing the inert layer thickness to a = 8 mm results in the failure of the detonation reinitiation and thereby continuous decay of

the leading shock speed. This is because the strength of the transmitted shock becomes too weak to trigger local autoignition and overdriven detonation afterwards for relatively large inert layer thickness. The above evolution of the leading shock speed is consistent with the idealized detonation reinitiation process across an inert layer presented in [13].

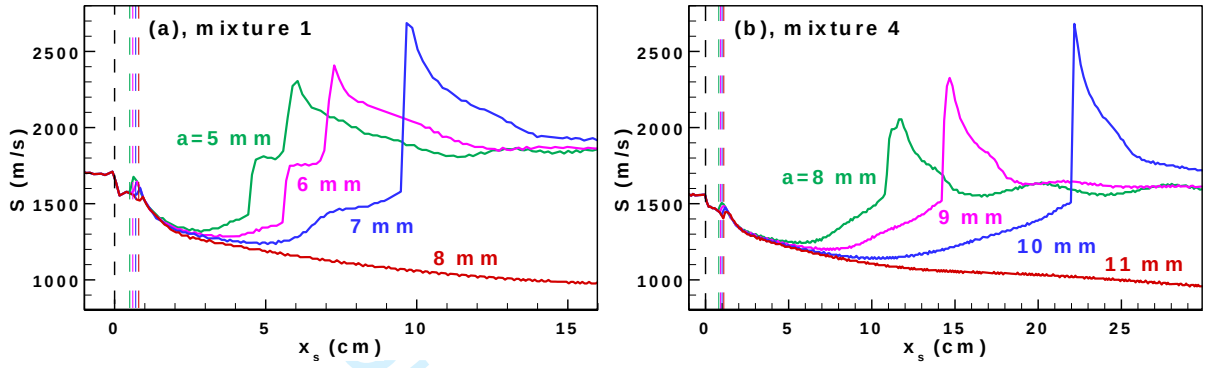

Fig. 2. Change of the leading shock speed with its position for mixtures 1 and 4.

Similar results are observed in Fig. 2(b) for mixture 4. Compared to mixture 1, mixture 4 has much higher N_2 dilution, and thereby weaker detonation strength. However, Figs. 2(a) and 2(b) shows that the critical inert layer thickness of mixture 4 is larger than that for mixture 1. This is counterintuitive since a weaker detonation is expected to be quenched by a thinner inert layer. Table 1 shows that the induction lengths of mixture 1 and mixture 4 are respectively $l_i = 1.49$ mm and $l_i = 4.31$ mm. The results in Fig. 2 indicate that a_c increases with l_i. Therefore, reinitiation for detonation propagating across an inert layer is more closely related to the induction length than the detonation strength.

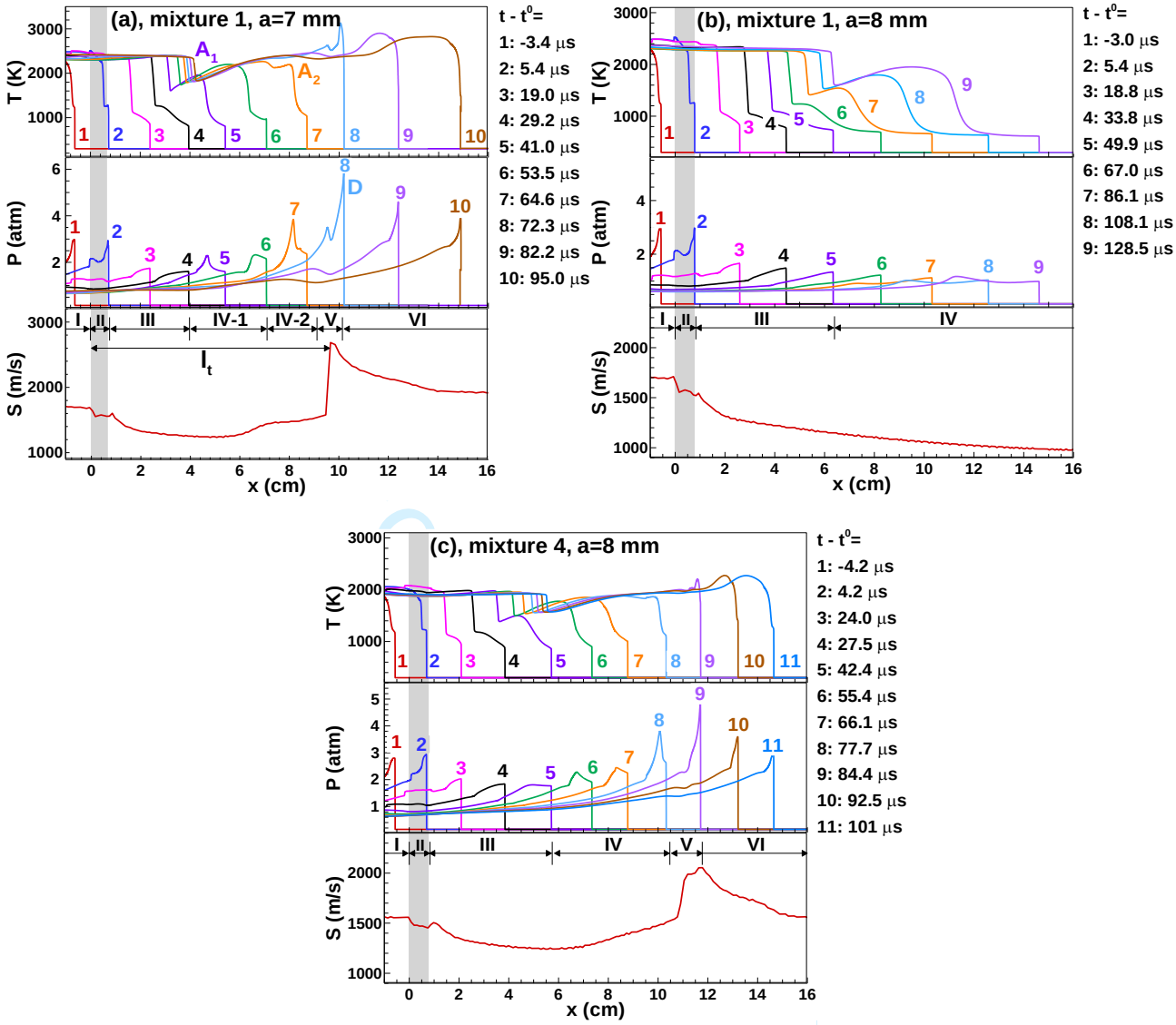

Fig. 3. Temporal evolution of temperature and pressure distributions and leading shock speed.

Figure 3 shows the details on the detonation transmission involving shock-reaction decoupling, local autoignition and detonation reinitiation. The gray zone in Fig. 3 corresponds to the inert layer. Moreover, Fig. 3 shows different states: I, steady detonation propagation; II, detonation quenching in the inert layer; III, shock attenuation; IV-1, first autoignition; IV-2, second autoignition; V, development of overdriven detonation; and VI, transition to steady detonation propagation. In Fig. 3, A1 represents the first autoignition, A2 the second autoignition and D detonation.

Figure 3(a) shows that for mixture 1 with a = 7 mm (corresponding to the blue line in Fig. 2a), after entering the inert layer, shock-reaction decoupling is observed at t-t^0 = 5.4 μs (line #2 in Fig. 3a). Here t^0 represents the time when

the detonation enters the inert layer at x = 0 cm. The distance between the leading shock and reaction front further increases and reaches its maximum value of 14.1 mm at t-t^0 = 29.2 μs (line #4), which is one order larger than the induction length l_i = 1.49 mm for mixture 1. Moreover, the peak pressure continuously decreases as the transmitted shock propagates downstream the inert layer, which corresponds to continual attenuation of leading shock speed after it passes across the inert layer. However, around t-t^0 = 41 μs (line #5), the first autoignition, A1, occurs and induces a rapid increase in both peak pressure and leading shock speed. At t-t^0 = 64.6 μs (line #7), the secondary autoignition, A2, happens. Consequently, detonation reinitiation is achieved and the leading shock speed abruptly accelerates at t-t^0 = 72.3 μs (line #8). The overdriven detonation forms and its peak pressure is around 6 atm, which is much higher than the pressure of the von Neumann spike P_{VN} = 3.9 atm. At t-t^0 =95 μs (line #10) the detonation is fully developed.

When the inert layer thickness is increased to a = 8 mm for mixture 1 (red line in Fig. 2a), Fig. 3(b) shows that the distance between the leading shock and reaction front reaches 24.7 mm at t-t^0 = 49.9 μs (line #5 in Fig. 3b), which is much larger than 14.1 mm for mixture 1 with a = 7 mm, shown in Fig. 3(a). Although autoignition occurs behind the leading shock at t-t^0 = 67 μs (line #6), the autoignition induced reaction front cannot couple with the leading shock. Consequently, there is no detonation reinitiation and the detonation is quenched by the inert layer.

When the nitrogen dilution is increased to s = 7 (mixture 4) while the inert layer thickness is still a = 8 mm (green line in Fig. 2b), the overall processes are similar to those in Fig. 3(a) and detonation reinitiation occurs. Different from the result for mixture 1 with a = 8 mm, Fig. 3(c) shows that the autoignition occurs at t-t^0 = 55.4 μs (line #6 in Fig. 3c). The autoignition-induced reaction front accelerates and couples with the leading shock at t-t^0 = 84.4 μs (line #9). This is because the leading shock speed is relatively small compared to that for mixture 1 and thereby the reaction front can catch up with the leading shock more easily. Besides, the autoignition position is close to the leading shock and their distance is around 6.1 mm, which is close to the induction length, l_i = 4.31 mm, for mixture 2. Consequently, for the same inert layer thickness of a = 8 mm, successful detonation reinitiation occurs in mixture 2, which has higher dilution and longer induction length than mixture 1.

As depicted in Fig. 3(a), there is a transition distance, l_t, after which the over-driven detonation develops. The transition distance is defined as the distance between the position where the inert layer starts to appear and the position where the sharp increase of shock speed occurs (i.e., the over-driven detonation develops). Figure 4 summarizes the change of the transition distance with the inert layer thickness from by 1D simulations, in which the dashed vertical lines correspond to the critical inert layer thickness. The transition distance is shown to increase with the inert layer

thickness for both mixtures 1 and 4, which is consistent with experimental results in [15]. For larger inert layer thickness, the transmitted shock after the inert layer becomes weaker. Consequently, a longer transition distance is needed to induce autoignition in the unburned mixture compressed by the transmitted shock and to achieve successful detonation reinitiation. Moreover, Fig. 4 shows that nitrogen dilution slightly increases the transition distance while it greatly increases the critical inert layer thickness from a_c = 7 mm for mixture 1 to a_c =10 mm for mixture 2.

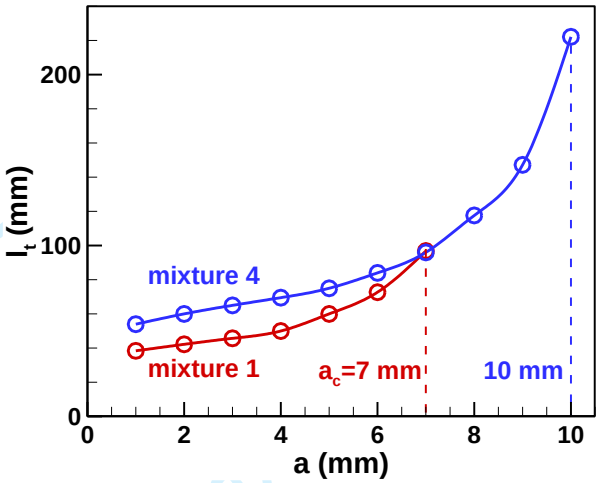

Fig. 4. Change of transition distance with the inert layer thickness from 1D simulations.

In summary, the above 1D results demonstrate that N_2 dilution increases the critical inert layer thickness. Similarly, the results on mixtures 4-6 (not shown here) indicates that the critical inert layer increases as the pressure decreases. This is because increasing N_2 dilution and reducing initial pressure both can increase the induction length (see Table 1) and thereby affects detonation propagation across an inert layer.

B. Two-dimensional Detonation Propagation

Then we considered the 2D detonation propagating across an inert layer. Six mixtures with different amounts of N_2 dilution and/or at different initial pressures (see Table 1) were all considered, though the results for mixtures 1 and 4 were mainly discussed here.

Figure 5 shows the numerical soot foils (which are obtained by recording the maximum pressure history in the computational domain) for mixtures 1 and 4 and two inert layer thicknesses. Regular cellular structure is fully developed and the peak pressure approaches to constant before the detonation enters the inert layer starting at x = 0 cm ($\Delta x = 150 l_i$). After entering the inert layer, the pressure at the triple points decreases substantially, indicating that

the reaction front starts to decouple with the leading shock. After passing the inert layer, the shock waves decay greatly and some triple points disappear, resulting in the formation of larger cells as shown in Fig. 5. A similar trend was also observed in [17]. For mixture 1 with the inert layer thickness of a = 7 mm, Fig. 5(a) shows that the peak pressure of cellular structures decays rapidly and the triple points almost disappear for $0 < x < 6$ cm. Around x = 9 cm, local explosions occur and the peak pressure increases and reaches 21 atm. Detonation reinitiation happens and cellular structures with the relatively small size appear. Then the cell size gradually increases; and finally the quasi-steady propagation is reached. When the inert layer thickness is increased to a = 10 mm, Fig. 5(b) shows that the detonation quenches after passing the inert layer and there is no detonation reinitiation. As nitrogen dilution increases (from mixture 1 with H_2:O_2:N_2 = 2:1:3.76 to mixture 4 with H_2:O_2:N_2 = 2:1:7), the cell size increases and peak pressure of cellular structure decreases, as detonation propagates across inert layer. This indicates that detonation quenches. Thereafter, successful detonation reinitiation is achieved by local explosions occurring around x = 11 cm. Therefore, Fig. 5 indicates that the increase in nitrogen dilution results in larger critical inert layer thickness. This trend is the same as was observed for the 1D case.

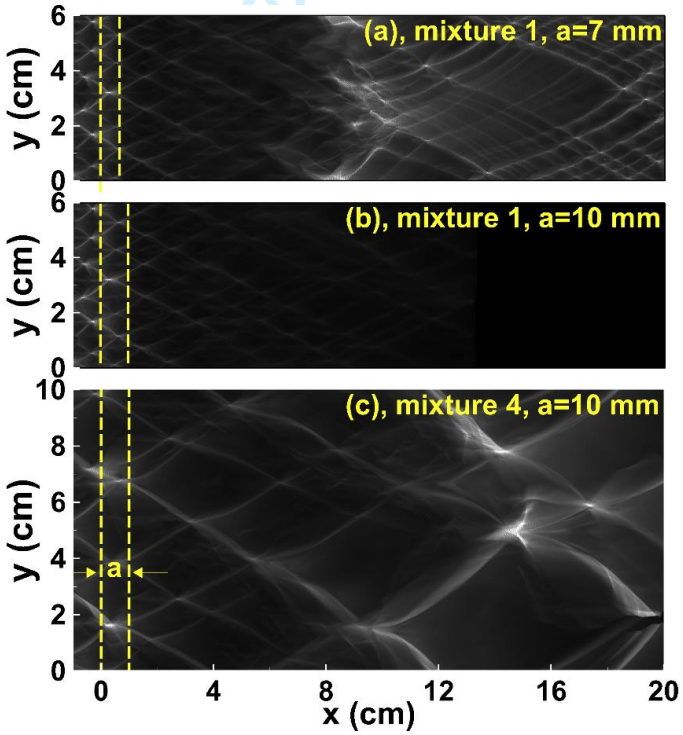

Fig. 5. Numerical soot foils for mixtures 1 and 4.

To show more details on detonation quenching and reinitiation processes, the evolution of temperature contours is

plotted in Fig. 6, in which SRD is shock-reaction front decoupling, SRC is shock-reaction front coupling, and E is explosion. The mixtures and inert layers are the same as those in Fig. 5. The detonation enters the inert layer (dashed line at x = 0 cm) at t-t_0 = 0 μs. Before entering the inert layer, in the regular cellular structure there is a relatively larger induction zone immediately after the incident shock since it is weaker compared to the Mach stem. The "unburned pockets" in these induction zones are brought into the inert layer and are consumed there by chemical reactions afterwards. The transmitted shock compresses the flammable mixture on the right side of the inert layer and increases its temperature to be above 1000 K, which induces local autoignition/explosion. Detonation reinitiation depends on whether an autoignition-induced reaction front couples with the transmitted shock. Comparison between Figs. 6(a) and 6(b) shows that the wider the inert layer, the longer the distance between the reaction front and the leading shock. Consequently, detonation reinitiation fails for the case with thicker inert layer. For mixture 4 with a = 10 mm, Fig. 6(c) shows that the local autoignition-induced reaction front is able to couple with the leading shock, which results in successful detonation reinitiation.

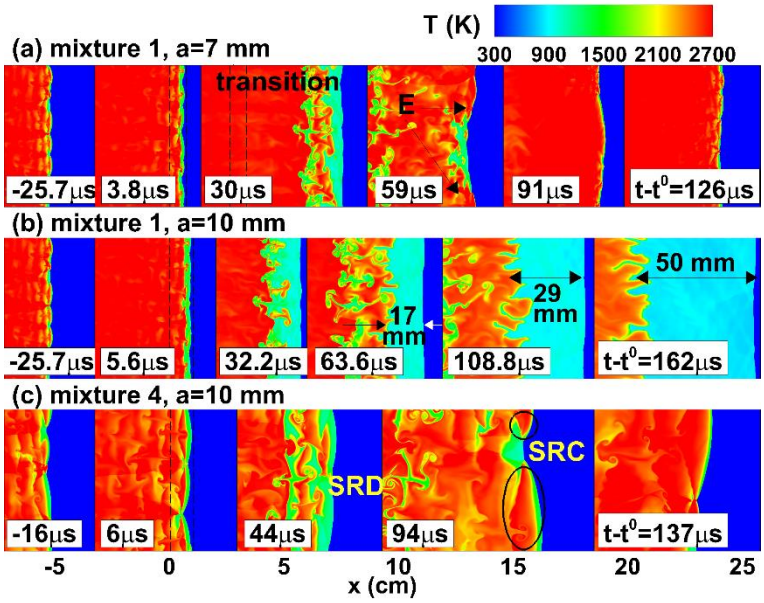

Fig. 6. Evolution of temperature contours for mixtures 1 and 4.

To further demonstrate the autoignition process, Fig. 7 plots the evolution of the enlarged density gradient, pressure and temperature contours for mixture 1 with a = 7 mm at t-t_0 = -4 μs (top row), 41 μs (middle row), and 56 μs (bottom row). In Fig. 7 M stands for Mach stem, I for incident shock, T for transverse wave, R for Richtmyer-Meshkov instability, A for autoignition, and E for explosion. At t-t^0 = -4 μs (i.e., before the detonation enters the inert layer), the

triple points consist of incident shock I, Mach stem M and transverse wave T. The reaction zone couples with the leading shock. As the detonation propagates across the inert layer, the leading shock collides with the interface between flammable H_2/air and inert nitrogen twice, which induces Richtmyer-Meshkov (RM) instabilities R_1 and R_2 as indicated in Fig. 7 (see the density gradient contour at t-t^0 = 41 μs). After interacting with the interface, the incident-leading shock splits into the transmitted and reflected shocks [14]. Besides, the density and acoustic impedance of the inert nitrogen are different from those of an H_2/air mixture, which changes the shock strength [36]. As shown by the temperature contour at t-t^0 = 41 μs, the reaction zone fully decouples with the leading shock and their distance is much larger than the induction length. The wrinkled reaction front is induced by RM instabilities. Meanwhile, the interaction of transverse waves T_1, T_2 and the RM instability R_2 results in the folding or superimposition of shock waves, which forms a local maximum of pressure and temperature and thereby induces the autoignition A_1 and subsequent explosion E_1 at t-t^0 = 41 μs. The local explosion interacts with the transverse wave T_2, which induces new autoignition A_2 and local explosion E_2 at t-t^0 = 56 μs, as shown in Fig. 7. Local explosions spread over the entire domain and a global explosion forms (see Fig. 6a). Finally, successful detonation reinitiation is achieved for this case.

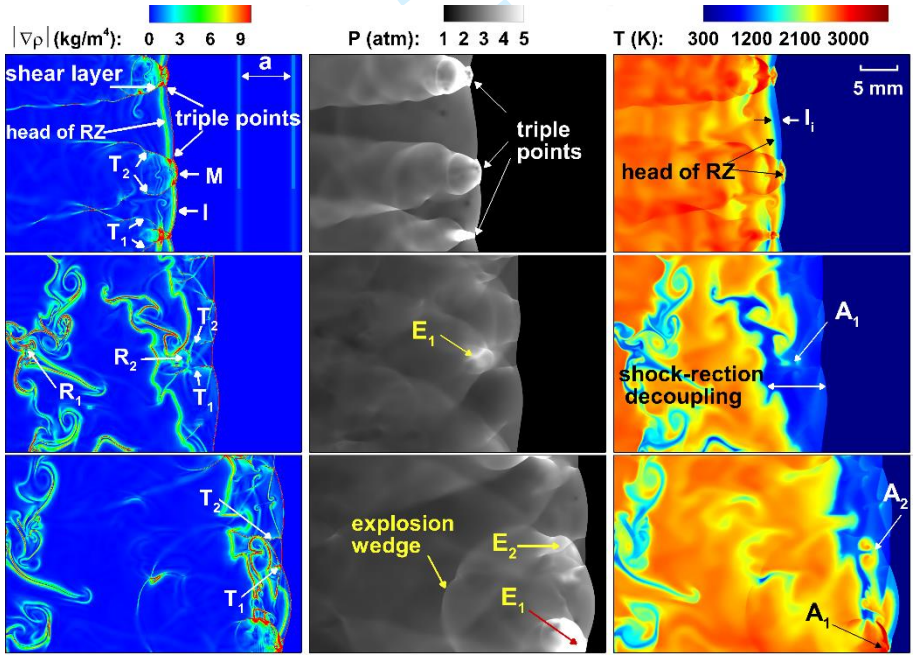

Fig. 7. Evolution of density gradient, pressure and temperature contours for mixture 1 with a = 7 mm.

The above results demonstrate that when the inert layer thickness is below some critical value, successful

detonation reinitiation is achieved after a transition process. To obtain the critical inert layer thickness, a_c, detonation propagating across a single inert layer with different thicknesses is simulated. The results for mixture 1 are shown in Fig. 8.

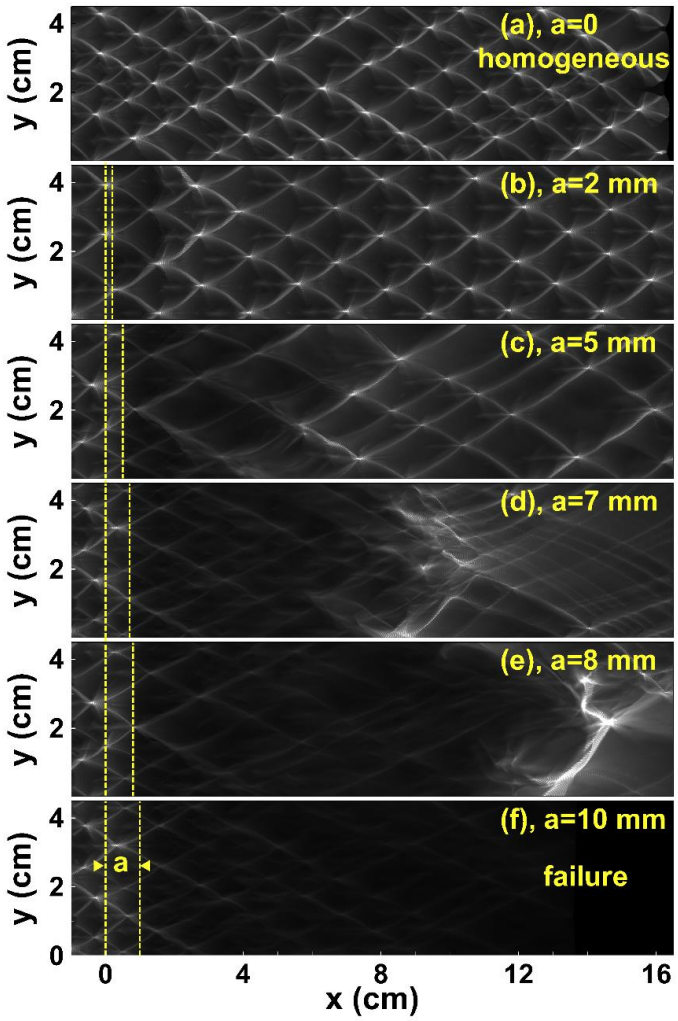

Fig. 8. Numerical soot foils for mixture 1 with different inert layer thicknesses.

The results for a homogenous mixture without inert layer, i.e., $a = 0$ is shown in Fig. 8 for comparison. For $a = 2$ mm, the inert layer has little influence on detonation propagation. The only difference is that the pressure at triple points slightly decreases after the inert layer. The cellular structure remains nearly the same as that for $a = 0$. When the inert layer thickness is increased to $a = 5$ mm, Fig. 8 shows that there is an obvious transition process, during which both the number of triple points and peak pressure decrease. For $a = 7$ and 8 mm, the cellular structures fully disappear during the transition process. For $a = 10$ mm, the detonation quenches without reinitiation. Note that the

result for a = 10 mm is independent of the computational domain length: detonation failure still occurs when the domain is extended.

Figure 8 indicates that the transition distance increase with the inert layer thickness. The transition distance from 2D simulations, l_t, is plotted in Fig. 9, which shows that l_t for the 2D case is smaller than that for the 1D case. This is because multi-dimensional effects (e.g., transverse waves and their interaction as shown in Fig. 7) can promote local autoignition and detonation reinitiation. Figures 4 and 9 show that the critical inert layer thickness is 7 mm and 8 mm respectively for 1D and 2D cases in mixture 1, and 10 mm and 20 mm respectively for 1D and 2D cases in mixture 4. This is because in the 1D case only the transmitted normal shock helps to induce detonation reinitiation, while in the 2D case the interaction among Mach stem, transverse wave and incident shock wave greatly promotes local autoignition/exposition and thereby enhances detonation reinitiation. Besides, from Fig. 9 we observed that the differences for both the transition distance and critical inert layer become larger as the amount of N_2 dilution increases (from mixture 1 red lines to mixture 4 blue lines). This indicates that the effects of transverse wave on detonation transmission increases with the amount of N_2 dilution.

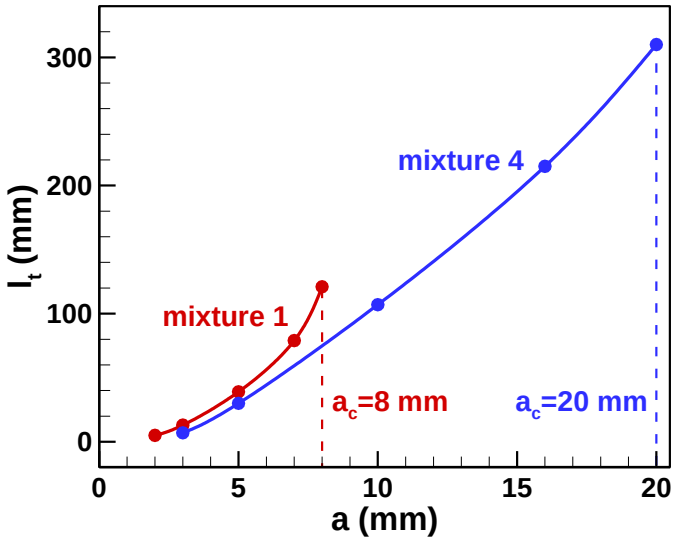

Fig. 9. Change of transition distance with the inert layer thickness from 2D simulations.

The above results show that nitrogen dilution increases the critical inert layer, a_c. Similarly, decreasing the initial pressure also increases a_c. Figure 10 shows a_c as a function of detonation cell size for six mixtures listed in Table 1. The line is a linear fit. Since the density of the inert layer is different from that of the reactive mixture, there is a change in shock impedance. We introduce an artificial inert mixture, H_2*/O_2*/N_2*, which has the same thermal properties and

acoustic impedance as the reactive $H_2/O_2/N_2$ mixture. Figure 10 also shows the results for an inert layer consisting of an artificial inert mixture, $H_2^*/O_2^*/N_2^*$. With the increase of nitrogen dilution (i.e., mixture 1→2→3→4 in Fig. 10) or decrease of initial pressure (i.e., mixture 6→5→4), both the critical inert layer thickness and detonation cell size increase. Therefore, the critical inert layer thickness is positively correlated to the detonation cell size or detonation induction length. Similar to the 1D case, the above 2D results also demonstrate that for larger cell size or induction length resulting from the higher nitrogen dilution or lower initial pressure, the self-sustained detonation can propagates under the condition which the reaction zone is relatively away from the leading shock. This is benefit of detonation propagating across inert layer and thus the larger critical inert layer thickness is obtained. Besides, Fig. 10 shows that the critical inert layer thickness for inert layer with artificial mixture, $H_2^*/O_2^*/N_2^*$, is close to that for an inert layer of pure nitrogen. Therefore, the change of acoustic impedance across the inert layer has little influence on detonation transition, at least for cases consider in this work.

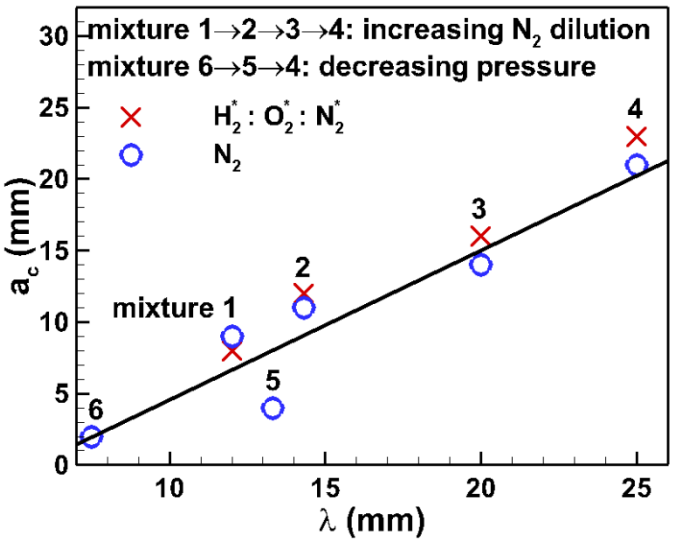

Fig. 10. The critical inert layer thickness and cell size for mixtures listed in Table 1.

In present work, the cell size based on the detailed chemistry [23] is quietly smaller than that measured values in experiments [37]. However, the qualitative relationship between the critical inert layer thickness and cell size/induction length can be obtained. Besides, present work only conducted 1D and 2D simulations, 3D cases allows additional interaction among shock waves.

IV. Conclusions

Detonation propagation across an inert layer was investigated through one- and two-dimensional simulations considering detailed chemistry for stoichiometric $H_2/O_2/N_2$ mixtures. Six mixtures with different amounts of nitrogen dilution and at different initial pressures were considered. This work focuses on assessing the effects of an inert layer on detonation transmission, especially the autoignition/explosion and detonation reinitiation processes. After the detonation enters the inert layer, the reaction front starts to decouple with the leading shock and some triple points disappear. The cellular structures fully disappear if the inert layer thickness is large enough. Successful detonation reinitiation occurs downstream when the inert layer thickness is below some critical value, i.e., $a < a_c$. The interaction of transverse waves, reactive-inert layer interface and instabilities jointly induces local autoignition/explosion and detonation reinitiation.

The nitrogen dilution and initial pressure greatly affect the detonation propagating across the inert layer. The critical inert layer thickness was found to be positively correlated to the detonation cell size or induction length. With the increase of nitrogen dilution or decrease of initial pressure, the induction length and cell size of detonation become larger, which unexpectedly results in the larger critical inert layer thickness. Therefore, counterintuitively a thicker inert layer is required to quench a weaker detonation (with more nitrogen dilution or with lower energy density at lower pressure). Moreover, the critical inert layer thickness for the 1D case was found to be lower than that for the 2D case since interaction among shock waves occurring in the 2D case rather than the 1D case promotes local autoignition/exposition.

It is noted that the simplified model considered here is far from practical cases using inert layers to quench detonations. For example, the inert gas is not static and it mixes with the flammable gases. The present mixture has regular detonation cell structure. For detonations with irregular cell structure, the reinitiation after passing an inert layer might be easier. These need to be explored in future studies. Besides, periodic boundary conditions in the direction normal to the detonation propagation were used in this study. As mentioned before, in practice the detonation propagates in a finite domain with physical confinement. Therefore, in future works it would be interesting to take into account the confinement effect. Furthermore, there exists the third dimension which allows additional interaction among shock waves. The effects of inert layers on detonation propagation need to be studied through 3D simulations in future works. Besides, in real propulsion systems, there is strong turbulence

which might affect the detonation structure (e.g., to broaden the reaction zone) as well as the inert layer. Consequently, the interaction between detonation and inter layer is affected by the turbulence. The dependence of the critical inert layer thickness and detonation reinitiation on the turbulence intensity needs to be investigated in future works.

Funding Sources

This work was supported by the National Natural Science Foundation of China (Nos. 52176096).

References

[1] Abdin, Z., Zafaranloo, A., Rafiee, A., and Khalilpour, K. "Hydrogen as an energy vector," *Renewable and Sustainable Energy Reviews* Vol. 120, 2020, p. 109620. https://doi.org/10.1016/j.rser.2019.109620

[2] Sánchez, A. L., and Williams, F. A. "Recent advances in understanding of flammability characteristics of hydrogen," *Progress in Energy and Combustion Science* Vol. 41, 2014, pp. 1-55. https://doi.org/10.1016/j.pecs.2013.10.002

[3] Han, W., Huang, J., and Wang, C. "Pulsating and cellular instabilities of hydrogen–oxygen detonations with ozone sensitization," *Physics of Fluids* Vol. 33, No. 7, 2021, p. 076113.

[4] Xu, Y., Zhao, M., and Zhang, H. "Extinction of incident hydrogen/air detonation in fine water sprays," *Physics of Fluids* Vol. 33, 2021, p. 116109. https://doi.org/10.1063/5.0055080

[5] Chen, X., Bttler, H., Scholtissek, A., Hasse, C., and Chen, Z. "Effects of stretch-chemistry interaction on chemical pathways for strained and curved hydrogen/air premixed flames," *Combustion and Flame* Vol. 232, 2021, p. 111532. https://doi.org/10.1016/j.combustflame.2021.111532

[6] Zhang, W., Kong, W., Sui, C., Wang, T., and Peng, L. "Effect of Hydrogen-Rich Fuels on Turbulent Combustion of Advanced Gas Turbine," *Journal of Thermal Science* Vol. 31, No. 2, 2022, pp. 561-570. https://doi.org/10.1007/s11630-021-1539-8

[7] Zhang, F., Zirwes, T., Wang, Y., Chen, Z., Bockhorn, H., Trimis, D., and Stapf, D. "Dynamics of premixed hydrogen/air flames in unsteady flow," *Physics of Fluids* Vol. 34, 2022, p. 085121. https://doi.org/10.1063/5.0098883

[8] Chen, X., Xie, S., Böttler, H., Scholtissek, A., Han, W., Yu, D., Hasse, C., and Chen, Z. "Effects of electrodes and imposed flow on forced ignition in laminar premixed hydrogen/air mixtures with large Lewis number," *Proceedings of the Combustion Institute* Vol. 39, 2022, Accepted and in press.

[9] Abohamzeh, E., Salehi, F., Sheikholeslami, M., Abbassi, R., and Khan, F. "Review of hydrogen safety during storage, transmission, and applications processes," *Journal of Loss Prevention in the Process Industries* Vol. 72, No. 3, 2021, p. 104569. https://doi.org/10.1016/j.jlp.2021.104569

[10] Yang, F., Wang, T., Deng, X., Dang, J., Huang, Z., Hu, S., Li, Y., and Ouyang, M. "Review on hydrogen safety issues: Incident statistics, hydrogen diffusion," *International Journal of Hydrogen Energy* Vol. 46, 2021, pp. 31467-31488. https://doi.org/10.1016/j.ijhydene.2021.07.005

[11] Kuznetsov, M., Denkevits, A., Veser, A., and Friedrich, A. "Flame propagation regimes and critical conditions for flame acceleration and detonation transition for hydrogen-air mixtures at cryogenic temperatures," *International Journal of Hydrogen Energy* 2022, published online. https://doi.org/10.1016/j.ijhydene.2022.07.024

[12] Mi, X., Higgins, A. J., Ng, H. D., Kiyanda, C. B., and Nikiforakis, N. "Propagation of gaseous detonation waves in a spatially inhomogeneous reactive medium," *Physical Review Fluids* Vol. 2, No. 5, 2017, P. 053201. https://doi.org/10.1103/PhysRevFluids.2.053201

[13] Teodorczyk, A., and Benoan, F. "Interaction of detonation with inert gas zone," *Shock Waves* Vol. 6, 1996, p. 211-223. https://doi.org/10.1007/BF02511378

[14] Bull, D. C., Elsworth, J. E., McLeod, M. A., and Hughes, D. "Initiation of unconfined gas detonations in hydrocarbon-air mixtures by a sympathetic mechanism," *Progress in Astronautics and Aeronautics* Vol. 75, 1980, pp. 61-72. https://doi.org/10.2514/5.9781600865497.0061.0072

[15] Bjerketvedt, D., Sonju, O. K., and Moen, I. O. "The influence of experimental condition on the reinitiation of detonation across an inert region," *Progress in Astronautics and Aeronautics* Vol. 106, 1986, pp. 109-130. https://doi.org/10.2514/5.9781600865800.0109.0130

[16] Tropin, D., and Bedarev, I. "Physical and mathematical modeling of interaction of detonation waves with inert gas plugs," *Journal of Loss Prevention in the Process Industries* Vol. 72, 2021, p. 104595. https://doi.org/10.1016/j.jlp.2021.104595

[17] Tang Yuk, K. C., Mi, X. C., and Lee, J. H. S. "Transmission of a detonation wave across an inert layer," *Combustion and Flame* Vol. 236, 2022, p. 111769. https://doi.org/10.1016/j.combustflame.2021.111769

[18] Wang, Y., Huang, C., Deiterding, R., Chen, H., and Chen, Z. "Propagation of gaseous detonation across inert layers," *Proceedings of the Combustion Institute* Vol. 38, No. 3, 2021, pp. 3555-3563. https://doi.org/10.1016/j.proci.2020.07.022

[19] Chen, Z., Burke, M. P., and Ju, Y. "Effects of Lewis number and ignition energy on the determination of laminar flame speed using propagating spherical flames," *Proceedings of the Combustion Institute* Vol. 32, No. 1, 2009, pp. 1253-1260. https://doi.org/10.1016/j.proci.2008.05.060

[20] Chen, Z. "Effects of radiation and compression on propagating spherical flames of methane/air mixtures near the lean flammability limit," *Combustion and Flame* Vol. 157, No. 12, 2010, pp. 2267-2276. https://doi.org/10.1016/j.combustflame.2010.07.010

[21] Deiterding, R. "Block-structured adaptive mesh refinement-theory, implementation and application," *Esaim: Proceedings* Vol. 34, 2011, pp. 97-150. https://doi.org/10.1051/proc/201134002

[22] Deiterding, R. "High-resolution numerical simulation and analysis of mach reflection structures in detonation waves in low-pressure H_2-O_2-Ar mixtures: A summary of results obtained with the adaptive mesh refinement framework AMROC," *Journal of combustion* Vol. 2011, 2011, pp. 1-18. https://doi.org/10.1155/2011/738969

[23] Li, J., Zhao, Z., Kazakov, A., and Dryer, F. L. "An updated comprehensive kinetics model of hydrogen combustion," *International Journal of Chemical Kinetics* Vol. 36, 2004, pp. 566-575. https://doi.org/10.1002/kin.20026

[24] Zhao, W., Liang, J., Deiterding, R., Cai, X., and Wang, X. "Effect of transverse jet position on flame propagation regime," *Physics of Fluids* Vol. 33, 2021, p. 091704. https://doi.org/10.1063/5.0063363

[25] Huang, C., Wang, Y., Deiterding, R., Yu, D., and Chen, Z. "Numerical studies on weak and strong ignition induced by reflected shock and boundary layer interaction," *Acta Mechanica Sinica* Vol. 38, 2022, p. 121466. https://doi.org/10.1007/s10409-021-09011-x

[26] Luan, Z., Huang, Y., Deiterding, R., and You, Y. "On the evolutions of triple point structure in wedge-stabilized oblique detonations," *Physics of Fluids* Vol. 34, 2022, p. 067118. https://doi.org/10.1063/5.0090975

[27] Wang, Y., Movaghar, A., Wang, Z., Liu, Z., and Chen, Z. "Laminar flame speeds of methane/air mixtures at engine conditions: Performance of different kinetic models and power-law correlations," *Combustion and Flame* Vol. 218, 2020, pp. 101-108. https://doi.org/10.1016/j.combustflame.2020.05.004

[28] Su, J., Wu, Y., Wang, Y., Chen, X., and Chen, Z. "Skeletal and reduced kinetic models for methane oxidation under engine-relevant conditions," *Fuel* Vol. 288, 2021, p. 119667. https://doi.org/10.1016/j.fuel.2020.119667

[29] Wang, Y., Chen, Z., and Chen, H. "Propagation of gaseous detonation in spatially inhomogeneous mixtures," *Physics of Fluids* Vol. 33, No. 11, 2021, p. 116105. https://doi.org/10.1016/j.combustflame.2021.02.040

[30] Wang, Y., Han, W., and Chen, Z. "Effects of stratification on premixed cool flame propagation and modeling," *Combustion and Flame* Vol. 229, 2021, p. 111394. https://doi.org/10.1016/j.combustflame.2021.02.040

[31] Sato, T., and Raman, V. "Detonation structure in ethylene/air-based non-premixed rotating detonation engine," *Journal of Propulsion and Power* Vol. 36, No. 5, 2020, pp. 752-762. https://doi.org/10.2514/1.b37664

[32] Pal, P., Demir, S., and Som, S. "Numerical Analysis of Combustion Dynamics in a Full-Scale Rotating Detonation Rocket Engine using Large Eddy Simulations," *Journal of Energy Resources Technology* 2022, pp. 1-31. https://doi.org/10.1115/1.4055206

[33] Ng, H. D., and Lee, J. H. S. "Direct initiation of detonation with a multi-step reaction scheme," *Journal of Fluid Mechanics* Vol. 476, 2003, pp. 179-211. https://doi.org/10.1017/s0022112002002872

[34] Qi, C., and Chen, Z. "Effects of temperature perturbation on direct detonation initiation," *Proceedings of the Combustion Institute* Vol. 36, No. 2, 2017, pp. 2743-2751. https://doi.org/10.1016/j.proci.2016.06.093

[35] Faghih, M., Mével, R., He, Y., and Chen, Z. "Effect of 2-step energy release on direct detonation initiation by a point energy source in a rich H_2-NO_2/N_2O_4 mixture," *Combustion and Flame* Vol. 222, 2020, pp. 317-325. https://doi.org/10.1016/j.combustflame.2020.08.036

[36] Ishii, K., and Seki, K. "A study on suppression of detonation propagation by inert gas injection," *Proceedings of the 26th International Colloquium on the Dynamics of Explosions and Reactive Systems, Boston.* 2017.

[37] Kaneshige, M., and Shepherd, J. E. "Detonation database. Technical Report FM97-8, GALCIT, July " 1997.